Received: 17 June 2022 | Accepted: 5 December 2022

DOI: 10.1111/1462-2920.16300

RESEARCH ARTICLE

ENVIRONMENTAL MICROBIOLOGY Applied Microbiology International

Prokaryotic maintenance respiration and growth efficiency field patterns reproduced by temperature and nutrient control at mesocosm scale

Ashish Verma[1,2] | **Dennis Amnebrink**[3] | **Jarone Pinhassi**[3] | **Johan Wikner**[1,2]

[1]Department of Ecology and Environmental Science, Umeå University, Umeå, Sweden

[2]Umeå Marine Sciences Centre, Hörnefors, Sweden

[3]Centre for Ecology and Evolution in Microbial Model Systems – EEMiS, Linnaeus University, Kalmar, Sweden

Correspondence
Johan Wikner, Department of Ecology and Environmental Science, Umeå University, SE-901 87 Umeå, Sweden.
Email: johan.wikner@umu.se

Funding information
Kempe Foundation, Grant/Award Number: SMK-185; EU H2020-INFRAIA, Grant/Award Number: 731065; European Commission

Abstract

The distribution of prokaryotic metabolism between maintenance and growth activities has a profound impact on the transformation of carbon substrates to either biomass or CO_2. Knowledge of key factors influencing prokaryotic maintenance respiration is, however, highly limited. This mesocosm study validated the significance of prokaryotic maintenance respiration by mimicking temperature and nutrients within levels representative of winter and summer conditions. A global range of growth efficiencies (0.05–0.57) and specific growth rates (0.06–2.7 d^{-1}) were obtained. The field pattern of cell-specific respiration versus specific growth rate and the global relationship between growth efficiency and growth rate were reproduced. Maintenance respiration accounted for 75% and 15% of prokaryotic respiration corresponding to winter and summer conditions, respectively. Temperature and nutrients showed independent positive effects for all prokaryotic variables except abundance and cell-specific respiration. All treatments resulted in different taxonomic diversity, with specific populations of amplicon sequence variants associated with either maintenance or growth conditions. These results validate a significant relationship between specific growth and respiration rate under productive conditions and show that elevated prokaryotic maintenance respiration can occur under cold and oligotrophic conditions. The experimental design provides a tool for further study of prokaryotic energy metabolism under realistic conditions at the mesocosm scale.

INTRODUCTION

Aerobic respiration is one of the fundamental processes in marine ecosystems that consumes dissolved oxygen and may cause hypoxia and oxygen minimum zones (OMZs). Prokaryotic respiration constitutes approximately half of aerobic respiration and is thereby an important process in the context of marine ecosystem health (Carstensen et al., 2014; Diaz & Rosenberg, 2008; Robinson & Williams, 2005; Schmidtko et al., 2017). The bioenergetic cost for prokaryotic specific respiration (ρ) in an aquatic ecosystem can be attributed to energy spent on maintenance activities and biomass synthesis. The proportion of prokaryotic maintenance respiration (ρ_m) to ρ is particularly large under oligotrophic conditions (i.e. low prokaryotic specific growth rates, μ) (Pirt, 1982; Vikström & Wikner, 2019). Maintenance energy is potentially used for the regulation of internal pH, osmoregulation, macromolecular turnover, re-establishing ion gradients, proofreading, defence mechanisms and motility (Cajal-Medrano & Maske, 1999; Russell, 2007; van Bodegom, 2007). Vikström and Wikner (2019) pointed out that a change in ecosystem productivity will lead to

a shift between maintenance and growth-based respiration with a moderate increase in μ, resulting in a minor influence on total respiration. This may explain the relatively stable levels of prokaryotic respiration found in field studies (Maranger et al., 2005; Obernosterer et al., 2008).

Temperature and nutrients are major controlling factors for prokaryotic growth rates and respiration, thereby influencing ρ_m. Experimentally controlling these factors in a mesocosm experiment should enable reproduction of the relationship between ρ and μ observed in the field and in culture studies. Short-term incubation experiments have shown that temperature is the main controlling factor for bacterial biomass production and specific growth rates within the range 3°C to <20°C, in contrast to substrate additions (Shiah & Ducklow, 1994). Pomeroy and Wiebe (2001) reviewed several studies and concluded that temperature and substrate interact at all substrate-temperature levels to control prokaryotic growth rates. Studies of this interaction under natural aquatic conditions are, however, few and differ with temperature regime. At elevated temperatures increased bacterial biomass production, community respiration and phyto-bacterioplankton coupling during spring bloom has been demonstrated in a temperate zone, when winter water was subjected to warming (Hoppe et al., 2008). Similar results of warming with increasing growth rates of marine prokaryotes have been obtained in different mesocosm systems (von Scheibner et al., 2014; Wohlers et al., 2009; Wohlers-Zöllner et al., 2012). Reports of the global range of μ are scarce, but a compilation by Kirchman (2016) shows 0.06–2.7 d^{-1} as a current estimate for marine surface waters.

The prokaryotic growth efficiency (PGE) is the proportion of prokaryotic carbon demand used for prokaryotic biomass growth (del Giorgio & Cole, 1998). The global range of PGE is 0.05–0.6 in marine ecosystems (Obernosterer et al., 2008; Roland & Cole, 1999). Some reports, however, suggest that PGE can be just a few percent in ultraoligotrophic regions ranging from 0.01 to 0.08 (Gasol et al., 1998; Pedrós-Alió et al., 1999). PGE responds positively to ecosystem productivity and thus prokaryotic growth (del Giorgio, 2000). In contrast, PGE shows an inverse relationship with temperature in some studies (Apple et al., 2006; Rivkin & Legendre, 2001; Schimel et al., 2007). However, the pattern of a monotonic decrease in PGE with increasing temperature is not universal and is dependent on the temperature range under investigation, with a peak at 15°C (López-Urrutia & Morán, 2007). Sufficiency of inorganic nutrients (N and P) can promote a negative PGE–temperature relationship, while no relationship was found when inorganic nutrients were scarce (Berggren et al., 2010). Direct estimates of PGE from oligotrophic coastal waters are still limited (Alonso-Sáez et al., 2007; del Giorgio et al., 2011; Lee et al., 2009), but the low PGE values reported from many environments, as mentioned earlier, indicate that ρ_m is considerable.

The prokaryotic specific rate of substrate utilization (e.g. O_2) is related to the specific growth rate (μ) and maintenance energy (m), as shown in culture experiments with bacteria (Pirt, 1982). The levels of oxygen consumption and maintenance respiration in these experimental systems were regulated by the type of limiting nutrients under carbon-replete conditions. The highest m was observed under phosphorus limitation (i.e. a high C:P ratio). Significant ρ_m has recently been demonstrated in a subarctic estuary, applying a simplification of the Pirt model (Vikström & Wikner, 2019). Annual ρ_m accounted for 24% of ρ using coefficients from a linear model. This was based on a significant relationship between ρ and μ during the productive season (August), while oligotrophic conditions in late winter (April) resulted in a seemingly elevated ρ without a clear relationship to μ. This elevated contribution from ρ in the late winter season indicated higher maintenance requirements during famine at low temperature. Further investigation of ρ_m is required to better understand its influence on and regulation in the natural environment. An advanced understanding of ρ_m in natural ecosystems is motivated by both ecological and evolutionary concerns. A large share of energy spent on maintenance metabolism will also impose selective forces on associated activities from an evolutionary perspective.

To investigate how ρ_m varies in relation to a realistic and wide range of μ, we designed conditions mimicking late winter and summer conditions in a mesocosm experiment initiated during winter (February) with brackish water collected from the Baltic Sea. By using temperatures of 1 and 10°C, respectively, winter and summer temperatures representative of the mixed layer of a temperate environment were simulated. The addition of nutrients was used to simulate increased nutrient supply from protozoan and zooplankton excretion and sloppy feeding during late summer. We hypothesized that the winter conditions should lead to low μ and thus high ρ_m, while late summer conditions would provide low ρ_m at high μ. ρ_m was assumed to be described by the established relationship between ρ and μ (Vikström & Wikner, 2019). The overarching aim of this study was thus to experimentally reproduce, at the mesocosm scale, patterns of ρ observed in the field, enabling controlled investigation of ρ_m and its influence on PGE. The specific questions addressed were as follows: (1) How do winter and summer conditions reproduced in a mesocosm setup influence the relationship between prokaryotic specific respiration and specific growth rates? (2) How do temperature and nutrients in interaction control the range of prokaryotic specific growth rates, specific respiration and growth efficiency

observed in natural waters? (3) Is there a relationship between the specific growth rate, maintenance respiration and prokaryotic community composition?

EXPERIMENTAL PROCEDURES

Experimental treatments and mesocosm setup

To investigate the influence of temperature and nutrient status on prokaryotic maintenance respiration and growth efficiency, experimental conditions were designed to encompass their full seasonal range in temperate climate zones. Late summer conditions were therefore simulated in winter collected seawater in an indoor mesocosm system at Umeå Marine Sciences Centre, Umeå University, Sweden, situated in the Northern Bothnian Sea (63°34′ N, 19°50′ E). We performed a full factorial experiment with temperature and addition of dissolved organic matter (DOM) as treatment factors with a natural pelagic food web containing all trophic levels except fish. A total of four experimental treatments were set up with three replicates each (Table 1). The mesocosm facility consisted of 12 insulated black polyethylene tanks 2 m^3 in volume, 0.75 m in diameter and 5 m in height. Each mesocosm was filled with a mix of brackish seawater provided by tubes with inlets 800 m offshore at 2 and 8 m. All mesocosms were filled in parallel to avoid differences among them to limit variability with respect to inlet water. The water was first prefiltered using system filters of 2 mm mesh size to remove large zooplankton, fish, and debris. Temperatures of 1°C without the addition of labile DOM represented late winter conditions (treatment C), and 10°C with recurring additions of labile DOM simulated plankton excretion of nutrients (treatment TN) and late summer conditions in the Baltic Sea. This was designed to promote a full seasonal range of μ. Elevated temperature to 10°C without nutrient addition (treatment T) and recurring additions of DOM at 1°C (treatment N) provided a full factorial design, enabling determination of factor effects and interactions (Table 1).

TABLE 1 Experimental design for the mesocosm treatments (C, N, T and TN)

		Temperature (°C)	
Treatment		**1**	**10**
DOM (μmol C dm^{-3})	No addition	C	T
	+ 59	N	TN

Note: Temperature and nutrient addition (yeast extract, DOM) was the two factors in the experiment. Each treatment had triplicate mesocosm units. Natural DOM was present in all treatments. The added concentration of DOM shows the amount for the whole experiment made in aliquots every third day (cf. also Table S1 for other elements).

The whole water column was set at a uniform temperature using a temperature control system (Honeywell AB) with convective stirring (4 h turnover time) to avoid handling of the water layers. The addition of DOM in the form of yeast extract (Merck Millipore, granulated, cat. no. 1.03753.0500) was performed the day after filling the mesocosm, and later additions were performed every third day after sampling. The yeast extract was added at 477 mg $unit^{-1}$ after each sampling. For the whole experiment, this addition amounted to 59 μmol C dm^{-3}, or +17% of the ambient carbon concentration (Table 1). The total addition of nitrogen and phosphorus was 16 μmol N dm^{-3} and 1.0 μmol P dm^{-3}, respectively, as measured in the added yeast extract solution (Table S1). The DOM additions were mixed by pulling a PVC plate (30 × 30 cm) attached to a rope up and down the whole water column. The light climate simulated a gradual change during a day at the end of April with a solar spectrum provided by LED lamps (lightDNA R258 and software lightDNA8, Valoya, Finland). A 12:12 h light–dark cycle was applied. For all units, the quantum flux density at 1.5 m was set to the photosynthetic active radiation (PAR) level at 4 m at the end of April (SMHI, 2020), corresponding to 10 μmol m^{-2} s^{-1}. The software mimics the spectra of the sun based on latitude. The average irradiance at the surface was 122 μmol m^{-2} s^{-1}.

Sampling and analysis

The experiment was run for 27 days, and a total of eight samplings were performed with a frequency of two samplings per week in a randomized fashion. The first day of mesocosm filling was defined as label 'S', representing the starting community in the metabarcoding experiment, while the first addition of nutrients on the subsequent day was defined as Day 0. The light irradiance profiles of PAR were measured from the surface down to 4 m at each 0.5 m interval using a Licor LI1400 radiometer with a LI-193 spherical sensor (LI-COR®). The total sample volume collected for analysis of various variables was always ≤1.2% of the total mesocosm volume at all sampling days (based on max. 25 dm^3 from 2 m^3). Water samples were first collected in acid washed (1 mol dm^{-3} HCl) 25 dm^3 polycarbonate bottles from a hose connected to a mesocosm faucet at 1.5 m depth and were immediately transferred to walk-in climate control rooms maintained at in situ mesocosm temperatures (1 and 10°C) for prefiltration setup, sample collection and processing. The water samples were prefiltered through <1.2 μm and 142 mm polycarbonate filters (Isopore, Merck Millipore™) at −20 kPa to remove phytoplankton, heterotrophic nanoflagellates and other large organisms to measure variables at the prokaryotic level only. All the filtration units, silicon tubing, glass and polycarbonate bottles were first washed

and rinsed with 1 mol dm^{-3} HCl, followed by rinsing in Milli-Q water prior to use. After prefiltration, the samples were analysed for prokaryotic respiration, growth, abundance, and total dissolved carbon, nitrogen, and phosphorus. Due to the limitation of running only eight samples for prokaryotic respiration in the incubator box, the remaining four samples were run on the day after the 24 h period, considering them to be part of a single sampling only.

Prokaryotic respiration

The prokaryotic respiration rate estimates (PR) were determined by measuring oxygen in prefiltered samples (1.2 μm) with optodes during incubations as described earlier (Vikström & Wikner, 2019; Wikner et al., 2013) using an incubator box based on the Peltier element technique (±0.1°C). Four slots of the incubator box were set at 1°C, while the remaining four were set at 10°C. Briefly, 1 dm^3 sample bottles filled with <1.2 μm filtered seawater samples with a magnetic stirrer and optode stopper were inserted in the slot of the incubator box. The change in oxygen concentration was measured with an optode for 20 h. Respiration rates are derived using a quadratic polynomical function for the best accuracy and precision of oxygen consumption. The specific respiration rate (ρ) was calculated by dividing the prokaryotic respiration rate (PR) by the cell abundance (PA).

Prokaryotic growth

The prokaryotic growth rate (PG) was estimated in triplicate subsamples (<1.2 μm filtered) with one control based on the thymidine incorporation method (Fuhrman & Azam, 1982). Handling of samples was performed in temperature-controlled walk-in climate rooms. Radioactively labelled ^{3}H-thymidine (2 mm^3, 81 Ci $mmol^{-1}$, 25 nmol dm^{-3} final concentration; GE healthcare, Buckinghamshire, UK) was added to a 1 cm^3 sample and TCA-killed control for 1 h of incubation at the in situ temperature. An empirical thymidine conversion factor of 1.5×10^{18} mol^{-1} of incorporated thymidine was applied based on a compiled dataset from the Baltic Sea (Wikner & Hagström, 1999). The specific prokaryotic growth rate (μ) was calculated by dividing the growth rate (PG) by the cell abundance (PA).

Prokaryotic abundance

Estimation of prokaryotic abundance (PA) was performed using direct epifluorescence microscopy (Zeiss Axioscope 5, Plan-Apochromat 63×/1.4, oil, ∞/0,17, Zeiss GmBH Germany) according to Hobbie et al. (1977). Briefly, 15 ml falcon tubes were rinsed with sample water and fixed with 37% formaldehyde (2% final concentration). Sample aliquots (5 cm^3) were vacuum filtered on 0.2 μm black-stained polycarbonate filters (25 mm, DHI) and stained with acridine orange (10 mmol dm^{-3}, Sigma-Aldrich) for whole-cell labelling and accurate cell volume estimation. Cell abundance, morphology and biovolume were estimated using image analysis using neural network technology (Blackburn et al., 1998; LabMicrobe, Bioras™, Denmark). Cell volume was converted to cell carbon density according to the function described by Norland (1993) and Simon and Azam (1989).

Prokaryotic growth efficiency

Prokaryotic growth efficiency (PGE) was calculated based on the prokaryotic community growth rate (PG) and prokaryotic respiration rate (PR) variables as follows:

$$PGE = PG/PG + PR \quad (1)$$

where PG and PR are both in carbon units (μmol C $dm^{-3}d^{-1}$). A respiration quotient (RQ) of 1.0 was applied to convert O_2 consumption to carbon units (Reinthaler et al., 2006).

Nutrients and dissolved carbon

Prefiltered (<1.2 μm) water samples from each treatment were collected in 50 cm^3 falcon tubes prerinsed with Milli-Q water. Samples were filtered through 0.2 μm sterile filters (0.2 μm Supor filters: Pall Corporation), and the filtrate was stored in the dark at 4°C until further processing for nutrient and DOC estimation. Oxidation of stored nutrient samples (TDP and TDN) was performed by autoclaving in acidic potassium peroxodisulfate prior to analysis in a four-channel autoanalyser (QAAtro marine; Bran & Luebbe®, Sweden). The samples were stored in the dark at 4°C and analysed based on standard operating procedures from Umeå Marine Sciences Centre and the method by Grasshoff et al. (1999).

For DOC estimation, the stored filtered samples were acidified with 1.2 mol dm^{-3} HCl and purged with an inert gas for 10 min before analysis. Potassium hydrogen phthalate was used as a standard for calculating the carbon concentration. Analysis was performed using a Shimadzu TOC-5000 (Shimadzu Corporation, Kyoto, Japan), a high-temperature catalytic oxidation instrument with nondispersive infrared (NDIR) detection and a TOC-L instrument (Norrman, 1993; Sugimura & Suzuki, 1988).

Maintenance respiration

The Pirt model explaining the relationship between ρ and μ was simplified following a published method (Vikström & Wikner, 2019). The simplified model showed that the maintenance respiration (ρ_m) can be estimated either using Model II linear regression with a major axis loss function or the nonlinear, polynomic quadratic model depending on the fit of the data (equations 2 and 5, Vikström and Wikner (2019)). Model II regression was preferred, as it complies with the theory for maintenance respiration and gave a better coefficient of determination (r^2) than the nonlinear regression in our analysis. ρ is the measured per cell (specific) respiration consisting of both maintenance respiration (ρ_m) as the intercept on the *y*-axis and the prokaryotic respiration associated with prokaryotic community growth (expressed as bμ), where b represents the slope and μ refers to the measured cell-specific prokaryotic growth rate (Equation 2). Outliers were removed based on Cook's distance before proceeding with the regression analysis for all treatments.

$$\rho = \rho_m + b\mu \quad (2)$$

Metabarcoding of the 16S rRNA gene

Approximately, 2.5 dm^3 seawater was prefiltered through 3 μm pore size polycarbonate filters (GVS) and then filtered onto Sterivex filters (0.22 μm). Subsequently, 1.8 ml of TE-buffer was added, and samples were stored at −80°C until extraction. DNA was extracted using the FastDNA™ Spinkit for soil (MPbio) according to the manufacturer's instructions. Following extraction, the V3–V4 region of the 16S rRNA gene was amplified using the primers 341F and 805R (Herlemann et al., 2011) following the protocol of Hugerth et al. (2014). The samples were sequenced at NGI (Stockholm, Sweden) using the Illumina MiSeq platform and a 2 × 300 bp setup.

Statistical and bioinformatic analysis

The effects of temperature and the addition of nutrients on the response variables were tested using repeated measures analysis of variance (RMANOVA) with a generalized linear model. The measures were recorded in a repeated fashion within the different treatments using temperature and nutrient additions as fixed factors. Partial eta-squared (η^2) values were used to indicate the effect size for determining the amount of variation explained exclusively by a particular factor. No variable followed the assumption of Mauchly's test of sphericity ($p < 0.05$), so Greenhouse-Geiser correction was applied. The quantitative changes in the different variables were tested using trend analysis by simple linear regression or the Mann–Kendall trend test (Sen's slope) based on the distribution of the data. Differences among different treatments for all independent variables were tested using pairwise multiple comparison tests. Based on the Shapiro–Wilk test, the data were found to be normally distributed only for μ and PGE. Transformation based on inverse and natural logarithm failed to achieve normal distribution so independent sample k-median with a two-tailed test and Bonferroni correction was used, while in case of normally distributed data, a post hoc Tukey-HSD-test was applied. The standard error for PGE was calculated from sum of squared errors for PG and PR as reported earlier (Toolan, 2001). All statistical tests were conducted in SPSS software (IBM® SPSS® Statistics Version 25), and graphical outputs were generated in R software (Version 3.6.3; R Development Core Team, 2020) using the ggplot2 package (Wickham, 2016).

For sequence data, the resulting FASTQ files were denoised and taxonomically annotated using the nf-core/ampliseq pipeline (Straub et al., 2020). Briefly, sequence libraries were inspected using FastQC (v0.11.8; Andrews, 2011) and MultiQC (v1.9; Ewels et al., 2016), and primers were removed with Cutadapt (v2.8; Martin, 2011). Reads were trimmed to 259 (forward) and 199 (reverse) bp with QIIME2 (Bolyen et al., 2019), and the resulting sequences were denoised with QIIME2's DADA2 (Callahan et al., 2016) implementation and annotated against the Silva database (v.132; Quast et al., 2013). The resulting abundance and taxonomy tables were imported into R studio for further analysis using the vegan (Oksanen et al., 2020) and pheatmap (Kolde, 2019) packages. Pairwise Bray–Curtis distances were calculated on Hellinger-transformed counts using the RDA function from the vegan package. PERMANOVA was used to investigate the influence of treatments on the community using the adonis function from the vegan package. To identify statistically significant correlations between individual ASVs and maintenance respiration as well as prokaryotic growth, multiple Spearman correlations were run for all ASVs, and the p values were then corrected using Bonferroni correction. The correlation between community composition, maintenance respiration and specific growth rate was determined using the Mantel test.

RESULTS

Temporal dynamics in prokaryotic variables

Statistics for the different prokaryotic variables in all the treatments are presented in Table S2. The prokaryotic community growth rate (PG) and respiration rate (PR) showed a slight increase in the TN treatment after

the 3-day conditioning of the mesocosm units, while PA was similar between treatments (Figure 1). The TN treatment showed higher values in general during the experiment followed by the T treatment, while the N treatment and especially the control (C) remained low and comparably stable. A peak was observed for PG and PA at Day 17, while this was less clear for PR. Compared to the TN treatment, there was a slower gradual increase in PG in the T treatment until Day 20 (Sen's slope = 0.21, $n = 18$; $p < 0.001$), followed by a decline (Sen's slope = −0.54, $n = 9$; $p < 0.05$). A similar gradual increase was observed for PA in the T treatment but remained at the highest level among treatments to the end of the experiment. PR in the TN treatment had already reached a higher level on the first day of sampling (Day 3), and the average fold change was 5-fold higher than that in the other treatments (2.2–4.3) (Figure 1C). After the PR peaked in the TN treatment at Day 17, the values declined to a similar level as the other treatments at Day 24, despite recurrent nutrient addition (Sen's slope = −0.72, $n = 9$; $p < 0.05$). The T treatment showed a tendency ($0.05 < p < 0.10$) to increase PR until Day 6 (Sen's slope = 1.3, $n = 6$; $p = 0.06$) and then a gradual decline (Sen's slope = −0.12, $n = 21$; $p < 0.05$). PR in the C and N treatments remained at low and stable levels during the experiment (slope = 0.04, $n = 24$; $p > 0.05$).

The level of specific prokaryotic respiration (ρ) in the N treatment was highest during the second half of the experiment from Day 13, albeit with a weak tendency ($0.05 < p \leq 0.10$) to increase due to high variation between treatment replicates (Sen's slope = 0.21, $n = 15$; $p = 0.10$; Figure S1a). ρ in the control was stable and showed an increase toward the end of the experiment. The T treatment showed an 8.3-fold change in ρ, although the only significant increase was seen from Day 3 to Days 6 (Sen's slope = 1.08, $n = 6$; $p < 0.05$), followed by a significant decline (Sen's slope = −0.13, $n = 21$; $p < 0.05$) (Figure S1b). In the TN treatment, ρ started at a high level, showing a similar significant gradual decline from Day 10 (Sen's slope = −0.16, $n = 18$; $p < 0.05$) and was, together with the T treatment, lowest at the end of the experiment.

A rapid increase in μ in the T and TN treatments was observed from Days 3 to 6, and a decline was observed from Days 17 to 20, respectively (Figure S1b). μ was clearly highest from days 10 to 17 for TN treatment in contrast to the T treatment (paired *t*-test, $n = 9$, $p < 0.001$). On average, the TN treatment showed 1.6 times higher μ values than the T treatment (paired t-test; $n = 24$; $p < 0.05$). Among all the treatments, the average levels of μ remained lowest for the control (Table S2). μ in the N treatment showed a gradual increase, reaching 1.1 d^{-1} at Day 13, and

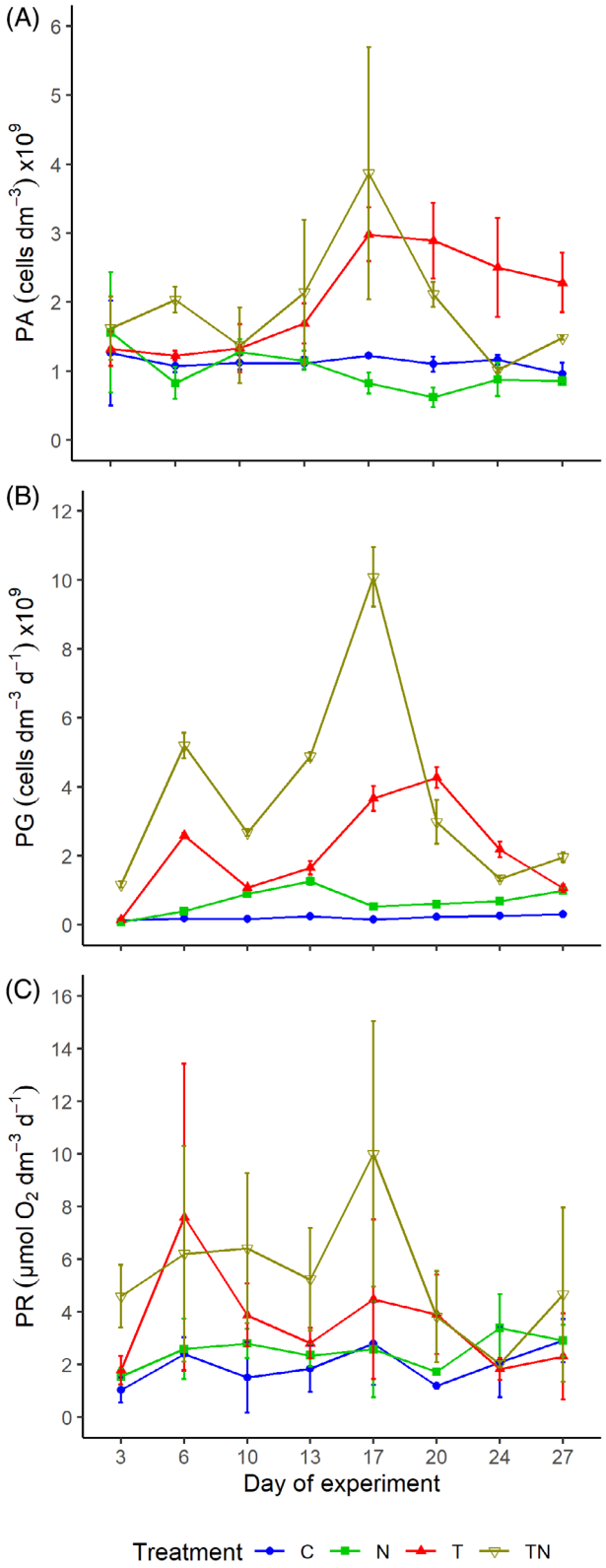

FIGURE 1 Temporal dynamics of (A) prokaryotic abundance (PA), (B) prokaryotic community growth rate (PG) and (C) prokaryotic community respiration (PR). The *x*-axis shows the time from start of the experiment, which is the same for all panels. Treatments are defined in Table 1. Error bars show 2 × S.E.M. for triplicate mesocosm units.

then stabilizing. The control sustained the lowest μ level with 2.6-fold variation (based on treatment average) throughout the experiment, followed by the TN treatment with a 4.1-fold variation. The N and T treatments showed the highest (18- to 20-fold) variation in μ due to the obtained minimum and maximum values (Table S2). The lower variation in the TN treatment compared to the N and T treatments was mainly due to a higher μ value in the first sampling.

TN showed higher PGE values than the other treatments, with a tendency to increase until Day 13 (slope = 0.02, $n = 12$; $p = 0.06$), followed by a significant decline (slope = −0.27; $n = 12$; $p < 0.05$) (Figure S1c). The N treatment also increased, albeit to a slightly lower level, until Day 13, while a gradual increase in PGE continued in the T treatment until Day 24 (slope = 0.02, $n = 21$; $p < 0.05$). The variation in PGE values was higher in the N and T treatments (8.5-fold) than in the C and TN treatments (2.7-fold).

Effect of temperature and nutrients

PR was positively influenced by temperature and showing a tendency to an effect by nutrients (Table 2). Temperature and addition of nutrients both independently and positively influenced the μ values, while ρ was positively influenced by nutrients alone (Table 2). The same pattern was also seen in the marginal mean estimation (Figure 2A,B).

PGE was enhanced by temperature alone, while the addition of nutrients showed a tendency to increase PGE, explaining a lower share of the variation than temperature (Table 2). The prokaryotic community growth rates were found to be positively influenced by both temperature and nutrient addition, while only temperature showed a significant positive effect on the prokaryotic community biomass. No synergistic or interaction effects of temperature and nutrients on any of the studied variables were observed (Table 2).

Patterns of ρ and μ

Based on the Model II linear regression, only the TN treatment showed a significant relationship between ρ and μ ($r^2 = 0.32$; Figure 3B). The y-intercept coefficient representing the ρ_m value was 0.45 fmol O_2 cell^{-1} d^{-1} (±0.37, 95% CI), and the linear slope coefficient (b) was 1.1 fmol O_2 cell^{-1} (±0.30, 95% CI). A nonlinear regression with the polynomic quadratic model was also applied to the data, but the coefficient of determination was found to be approximately half ($r^2 = 0.17$). Based on the better fit of the data and in accordance with current models (van Bodegom, 2007), the coefficients of the linear Model II regression were assumed

TABLE 2 RMANOVA with direction of significant treatment effects

Parameter	PA	PG	PR	ρ	μ	PGE
Temperature	↑ (0.00, 0.87)	↑ (0.00, 0.84)	↑ (0.00, 0.67)	n.s.	↑ (0.00, 0.92)	↑ (0.00, 0.81)
Nutrients	n.s.	↑ (0.01, 0.57)	↗ (*0.06*, *0.36*)	↑ (0.02, 0.51)	↑ (0.00, 0.84)	↗ (*0.07*, *0.37*)
Temperature × Nutrients	n.s.	n.s.	n.s.	n.s.	n.s.	n.s.

Note: The value in parenthesis signifies the probability of Type I error (p value) and the partial eta-squared value (η^2) variance explained by the independent variable. Arrows show ↑, significant positive effect ($p < 0.05$); ↗, tendency to show positive effect ($0.05 < p < 0.1$); n.s., non-significant.
Abbreviations: PA, prokaryotic abundance; PG, prokaryotic community growth rate; PGE, prokaryotic growth efficiency; PR, prokaryotic community respiration; RMANOVA, repeated measures analysis of variance; ρ, cell-specific respiration; μ, specific growth rate.

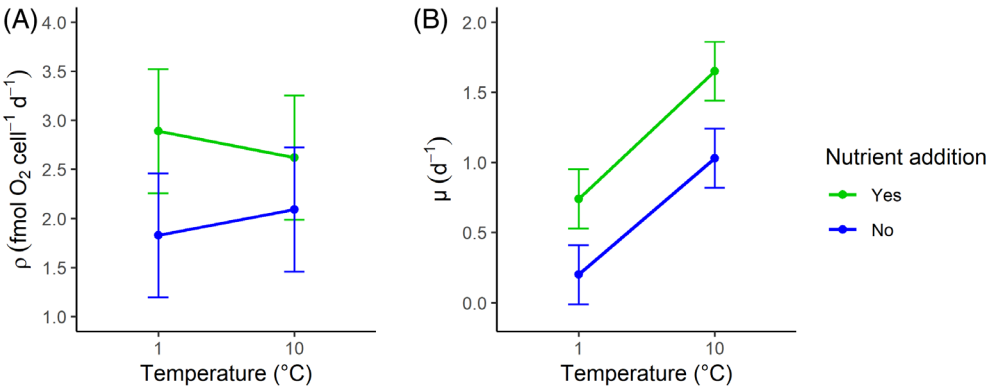

FIGURE 2 Marginal mean plots of (A) cell-specific respiration rate (ρ), and (B) specific growth rate (μ), based on repeated measures analysis of variance (RMANOVA) with nutrient and temperature levels. The nutrient levels are addition and no addition, and temperature levels refer to 1 and 10°C. Error bars show the marginal mean ± 95% confidence interval.

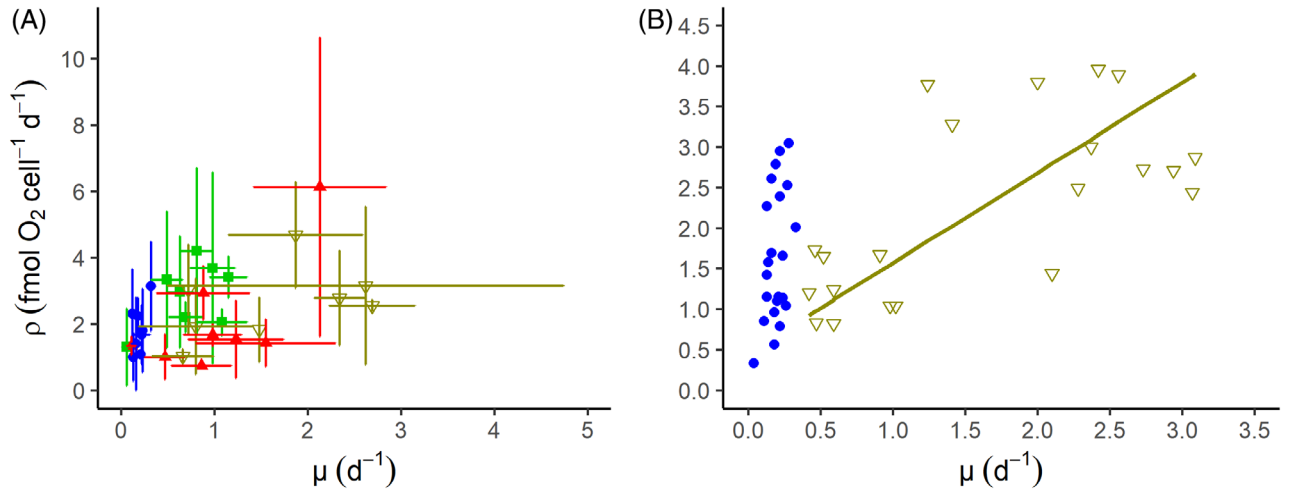

FIGURE 3 Cell-specific respiration rate (ρ) as a function of specific growth rate (μ) for (A) all treatments and (B) specific treatments. (A) Individual data points for each treatment representing the average of triplicates for eight samplings. Error bars show 2 × S.E.M. calculated from the triplicate treatment. (B) Scatterplot of ρ and μ for the C ($n = 22$) and TN treatments ($n = 21$) after outlier removal based on Cook's distance. The line represents the linear fit of the recorded data for the TN treatment (see Figure 1 for colour scheme of different treatments).

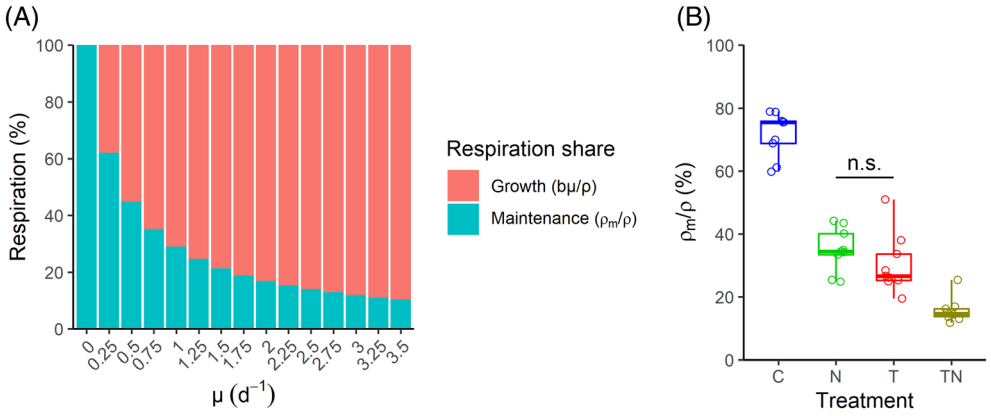

FIGURE 4 Share of (A) growth ($b\mu/\rho$) and maintenance respiration (ρ_m/ρ) relative to total respiration and (B) maintenance respiration (ρ_m/ρ) in different treatments. (A) Growth- and maintenance-related respiration as a function of prokaryotic specific growth rate (μ) in 0.25 d^{-1} bins based on the regression coefficients from the TN treatment dataset. (B) Boxplot representing the share of maintenance respiration (ρ_m/ρ) calculated from Days 10, 13 and 17 for all treatments assuming TN coefficients applicable ($n = 9$ each). The bar with n.s. label indicates lack of significant difference between covered treatments based on post hoc Tukey-HSD-test.

to be applicable to all treatments and used to calculate the proportion of prokaryotic maintenance respiration. The control showed a large range of ρ values within the narrow range of μ values observed, with a mean ρ of 1.8 fmol O_2 $cell^{-1}$ d^{-1} (±0.4, 95% CI; Figure 3).

Maintenance respiration modelling

A range of simulated μ values in individual treatment replicates between 0.1 and 0.25 d^{-1} was used for modelling the share of ρ_m relative to ρ, resulting in an exponential decrease in ρ_m with a corresponding increase in μ values (Vikström & Wikner, 2019, figure 4). The calculated ρ_m/ρ values showed an exponential increase with decreasing μ and were >50% for values of μ less than 0.4 d^{-1} (Figure 4A). To select time points reflecting clear treatment effects for μ after equilibration of the mesocosm system, Days 10 (third sampling), 13 (fourth sampling) and 17 (fifth sampling) were used to calculate ρ_m/ρ for all treatments (Figure 4B).

The selection of Days 10, 13 and 17 was motivated by a large difference in μ between the control and the TN treatment (paired *t*-test, $n = 9$; $p < 0.001$) and a low within-treatment variability. This would enable the study of microbial metabolism associated with a high proportion of maintenance respiration. It was further assumed that the coefficients derived from the TN treatment were applicable to the other treatments. Based on Days 10, 13 and 17, the median ρ_m/ρ values were found to be higher for the C treatment (75%), followed by the N (34%), T (27%) and TN treatments (15%) ($n = 9$ each;

Figure 4B). Moreover, the median ρ_m/ρ values based on all sampling points per treatment also indicated a higher share of maintenance in the control (68%, $n = 22$), followed by N (34.3%, $n = 24$), T (33.9%, $n = 21$), and TN (22.4%, $n = 21$) (data not shown). By multiple pairwise comparisons of ρ_m/ρ among the different treatments, these were found to be significantly different based on a post hoc Tukey-HSD test ($n = 9$ each, $p < 0.05$), except between the N and T treatments. The corresponding average μ values for Days 10, 13 and 17 were 0.2, 0.8, 1.0, and 2.4 d^{-1} for the C, N, T and TN treatments, respectively ($n = 9$ each).

Patterns of PGE

The observed range of prokaryotic growth efficiencies (PGEs) for all treatments was 0.05–0.57. PGE was found to be lowest in the control and N treatments (Figure 5A). The average values of PGE in each treatment were 0.12, 0.23, 0.37 and 0.40 for the C, N, T and TN treatments, respectively (Figure S1c and Table S2). All pairwise differences between treatments were found to be statistically significant except for the T and TN pair (Tukey's HSD post hoc test, $n = 24$ each, $p < 0.05$). The variation in PGE over the course of the experiment within treatments was considerable, especially in the T treatment. PGE showed a significant linear relationship with μ in the N, T and TN treatments and statistically significant r^2 values corresponding to 0.33, 0.35 and 0.52, respectively (Figure 5B and Table S3). All treatments and data points combined showed a significant linear fit ($n = 95$, $r^2 = 0.49$). A linear relationship between PGE and PG was also significant for each treatment except C. Model II fit showed significant r^2 values of 0.78, 0.51, and 0.54 for N, T, and TN, respectively. All data combined showed a significant linear fit ($n = 94$, $r^2 = 0.53$), but a better fit for the data was observed using the square root function as presented in Equation (3) ($n = 94$, $r^2 = 0.70$).

$$\mathrm{PGE} = 0.004 + 0.351 \times [\mathrm{sqrt}\,(\mathrm{PG})] \quad (3)$$

The calculation of PGE as reported by del Giorgio and Cole (1998), their equation 3, resulted in a lower r^2 value of 0.52 ($n = 94$).

Prokaryotic community composition analysis

The 16S rRNA gene analysis showed that the prokaryotic community composition diverged over time in the treatments compared to the control (Figure 6). The C-treatment remained rather stable and was characterized by a temporary increase in the *Methylophilaceae* family and an increase in *Burkholderiaceae* until Day 17. In the N-treatment, *Burkholderiaceae* rapidly increased until Day 13 and together with *Flavobacteriaceae* came to dominate the community. In the T-treatment, distinguishing features were a quick increase in *Nitrincolaceae* (up to 20%) on Day 8, followed by an increase in *Ilumatobacteraceae* from Day 17 onwards (reaching 25%). In the TN treatment, *Flavobacteriaceae* made up ~15% from Days 10 to 24. During this period, there were transient increases in *Nitrincolaceae*, 'Unknown' and *Sporichtyaceae*.

Further insight into community composition dynamics was obtained from a PCA plot (Figure 7). This showed a close clustering of all control samples together with starting community (S) and Day 6 samples from the T and N treatments (the TN samples had diverged already by Day 6). From Day 10 onwards, the

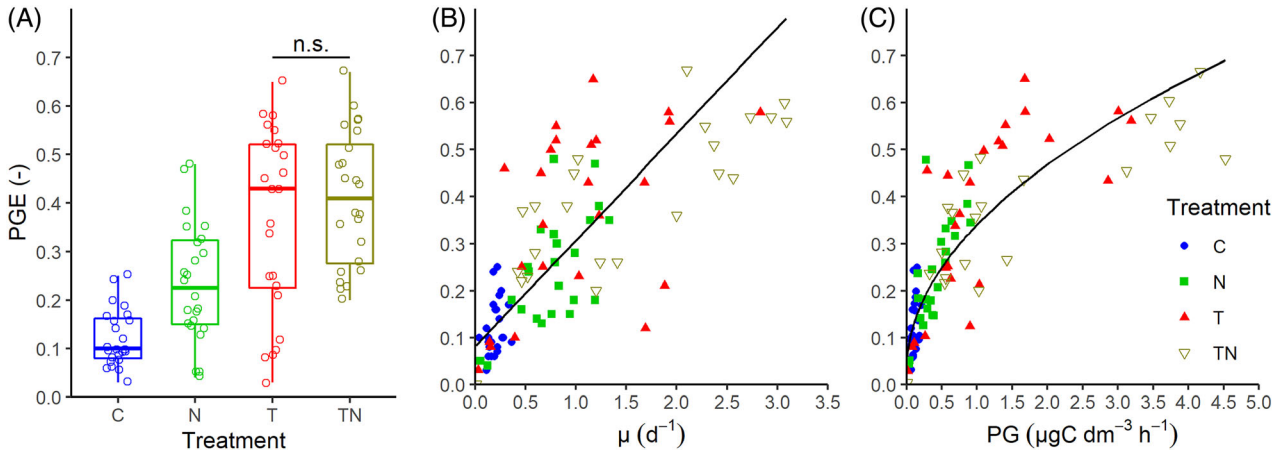

FIGURE 5 (A) Prokaryotic growth efficiency (PGE) in all treatments and its relationship to (B) specific growth rate (μ), and (C) prokaryotic community growth rate (PG). (A) Boxplot represents the distribution of PGE ($n = 24$, each treatment). The comparison between T and TN treatment based on post hoc Tukey-HSD-test is non-significant as shown by the bar above both treatments with n.s. label. (B) Relationship between PGE and μ for all treatments with Model II linear fit. (C) Relationship between PGE and PG for all treatments with a nonlinear fit.

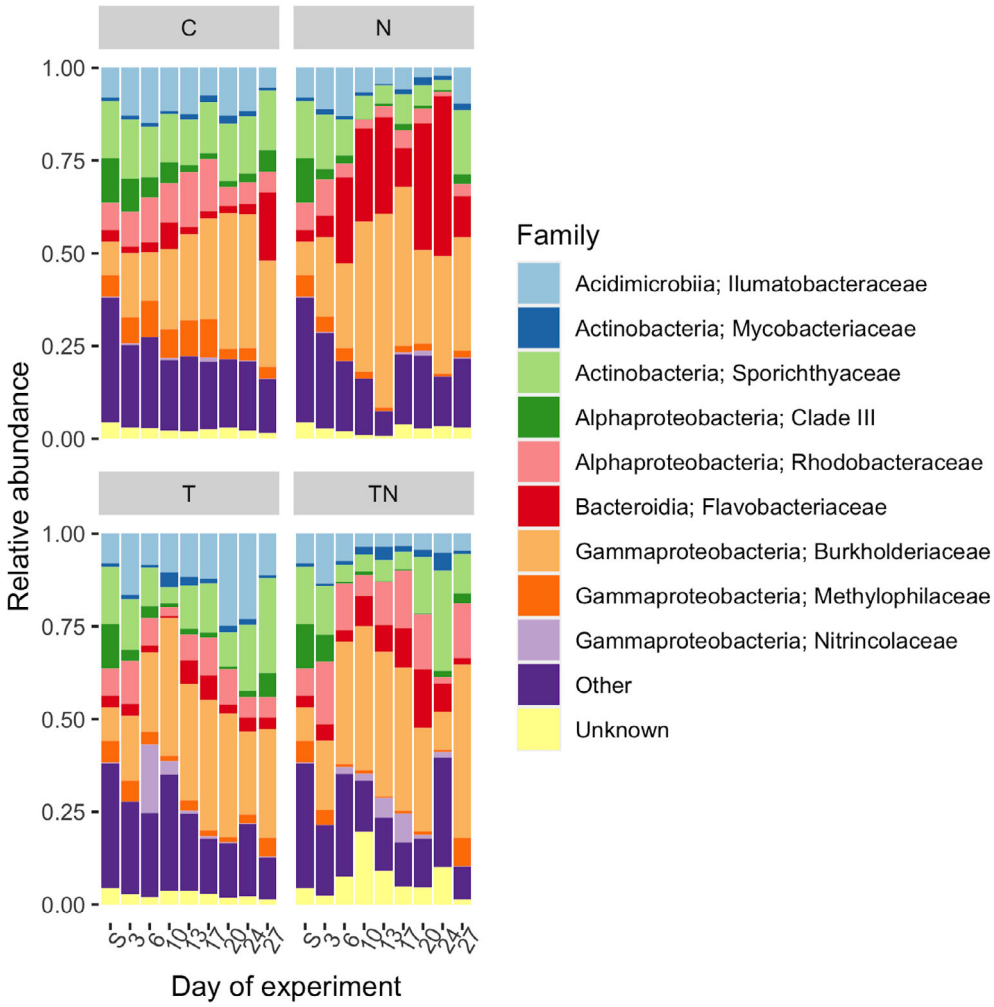

FIGURE 6 Relative abundance of taxa at the family level in the different treatments; family names are preceded by class-level taxonomy. The label 'S' on the *x*-axis represents the starting prokaryotic community on the first day of mesocosm filling.

samples deviated substantially so that they formed clusters essentially separating the treatments. In general, the treatments were most dissimilar from the starting community from Days 10 to 24. On Day 27, a large spread was seen among the C and N treatment replicates.

To identify the individual populations driving the dynamics in community composition, we investigated the patterns of the 50 most abundant amplicon sequence variants (ASVs), which accounted for 73% of the total community (Figures 6 and S2). The C-treatment showed high abundances of ASVs belonging to *Methylophilaceae* (ASV14, reaching 7.9% relative abundance) and *Rhodobacteraceae* (ASV3) until Day 17, followed by an increase in *Burkholderiaceae* ASVs (ASV1 and −4). The N treatment was characterized by a cluster of several *Burkholderiaceae* and *Flavobacteriaceae* ASVs generally showing a high relative abundance from Day 6 onwards. The T-treatment included an early rise in ASV15 (*Nitrincolaceae*), peaking at 17% relative abundance, followed by three *Burkholderiaceae* ASVs (ASV23, −2 and −16 peaking during Days 12–26), and an increase in *Ilumatobacteraceae* ASVs (ASV11 and −5) during Days 20 and 24. The TN treatment was characterized by a group of six taxonomically diverse ASVs that were abundant from Days 6 to 17. These included ASVs belonging to *Flavobacteriaceae* (ASV28), *Nitrincolaceae* (ASV15), *Rhodobacteraceae* (ASV7) and *Burkholderiaceae* (ASV2 and −16).

Statistical analysis showed that prokaryotic community composition was significantly different between treatments (PERMANOVA, $R^2 = 0.17$, $P = 0.001$), which was further determined using pairwise treatment comparisons for all treatment pairs (Table S4). Furthermore, community composition was positively correlated with maintenance respiration (Mantel test, Spearman's; $r = 0.17$, $p = 0.002$). ASVs positively correlated with high maintenance respiration (Spearman's; $r > 0.53$; Bonferroni-corrected $p < 0.05$) were found to be most prominent in the C-treatment (Table S5). In contrast, ASVs positively correlated with μ (Spearman's; $r > 0.4$;

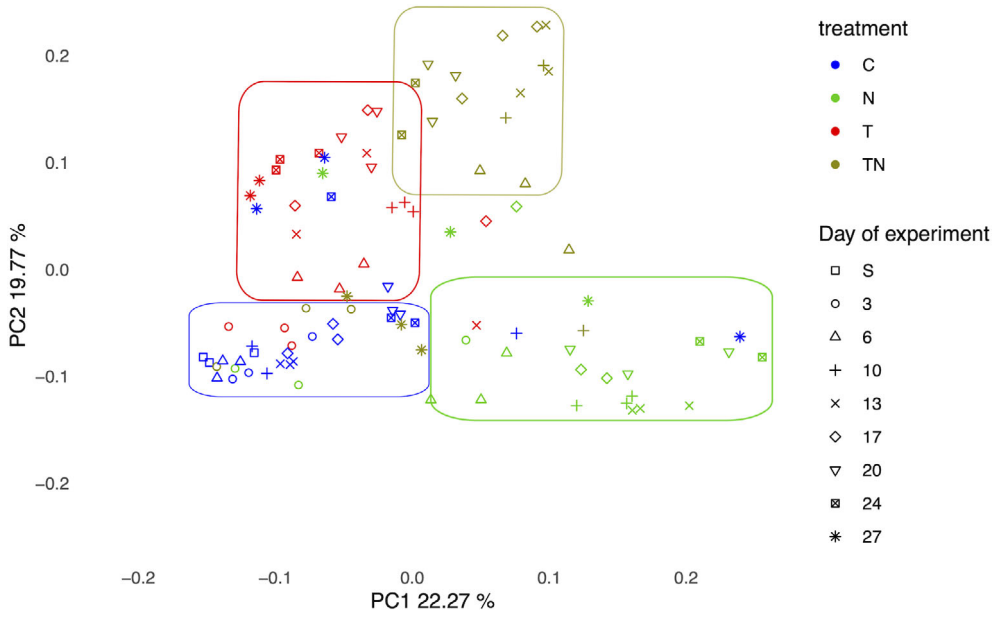

FIGURE 7 Principal component analysis (PCA) depicting prokaryotic communities of different treatments. Squares are added to help the reader identify the clustering of treatments.

Bonferroni-corrected $p < 0.05$) were abundant in the TN treatment (Table S5).

DISCUSSION

Global range of prokaryotic variables obtained

By conducting a mesocosm experiment starting during winter in a temperate estuary and promoting prokaryotic growth by increases in temperature and nutrients, we could reproduce a range of prokaryotic specific growth rates representative of values typically observed globally in the natural environment. This was also true for prokaryotic growth efficiency and respiration. Indeed, our measured range of PGE (0.05–0.57) and μ (0.06–2.7 d^{-1}) covered most of the global range reported in the literature (del Giorgio & Cole, 1998; Kirchman, 2016) (Table S2 and Figure S1a,b). This is a valuable insight for investigating ecological questions under controlled conditions and enabling larger sample volumes required for obtaining quantitative estimates of parameters such as metabarcoding and metatranscriptomics. The key for obtaining a natural range of values was the initiation of the experiment during the season with the lowest production and the coldest temperatures during winter in a temperate zone. This enables the use of temperature and nutrients for increasing productivity. The increase of mesozooplankton biomass, primarily in the TN treatment (10 times that in C), was evidence that applied treatment and the time frame of the experiment was sufficient to manifest summer conditions (data not shown). Reducing temperature in a developed plankton community during summer is a more challenging task. Making an experiment starting during the productive season would also require reducing the naturally high DOM concentrations. To our knowledge, mesocosm studies started during the temperate winter with a similar design have not previously been reported, although reports of elevated temperature and its effect on the winter bacterial and phytoplankton communities exist (Hoppe et al., 2008; von Scheibner et al., 2014, 2018).

Field patterns between reproduced ρ and μ

The pattern for ρ versus μ experimentally observed (Figure 3A,B) constitutes an important validation of recent field observations in the nearby estuary (Vikström & Wikner, 2019, figure 3). This mesocosm design thereby provides a tool for further investigations of maintenance respiration and other microbial metabolism. The control treatment matched well with the pattern of ρ versus μ observed in late winter, while the TN treatment showed a significant linear relationship observed during late summer in the field. The N and T treatments fell in between those seasons, but it is not straightforward to relate them to either spring or autumn, as both temperature and nutrient supply vary markedly during these seasons. From the TN treatment, we estimated coefficients where the y-intercept

of 0.45 fmol O_2 cell^{-1} d^{-1} (±0.37 95% CI) was close to and not significantly different from the field value of 0.32 (±0.18 95% CI) (Vikström & Wikner, 2019). The slope coefficient in the adjacent oligotrophic subarctic estuary (8.0 fmol O_2 cell^{-1}, ± 3.0 95% CI) was, however, clearly higher than that estimated in the mesocosm experiment (1.1 fmol O_2 cell^{-1}, ±0.3 95% CI) (Table S3). The slope coefficient is defined as

$$\left(\frac{1}{Y_g}-\frac{m'}{\mu_{m'}}\right), \quad (4)$$

by Pirt (1982, equation 6), where Y_g is the maximum growth yield at the realized growth condition, $\mu_{m'}$ is the maximum specific growth rate subtracted by the specific maintenance rate, *a,* and m' is the growth rate-dependent energy requirement at $\mu = 0$. As *a* is also a product of Y_g, an increase in the growth efficiency will decrease the slope. That is, better growth conditions will lead to less respiration required for a given increase in μ. Both the quality of bioavailable substrate and temperature are factors that contribute to better growth conditions for prokaryotes. The higher slope value observed in the adjacent oligotrophic subarctic estuary consequently indicates poorer growth conditions and a lower growth efficiency compared to the conditions over a global range of values obtained in the mesocosm setup. Replete growth conditions represented by the mesocosm system consequently require less energy spent by the prokaryote for a given increase in μ than an oligotrophic field site. The high nutritional quality and amount of yeast extract used to increase the DOM level created a global range of growth efficiency and covered half of the global range for prokaryotic growth rates but clearly higher levels than typical for the adjacent subarctic estuary (del Giorgio & Cole, 1998; Vikström & Wikner, 2019). This showed that the experimental conditions were relevant to the natural environment. Reduced amounts of added yeast extract or using a nutrient source closer to the stoichiometric composition of natural nutrients could be applied to achieve a lower slope value.

Assuming the relationship between ρ and μ in the TN treatment to be applicable to all treatments, a 5-fold difference in the share of ρ_m between the C (75%) and TN treatments (15%) was demonstrated (Figure 5A). The latter was closer to the annual average reported for a subarctic estuary (24%; Figure 4A; Vikström & Wikner, 2019). For comparability, the value based on a linear model was used from the field estimate. The influence of ρ_m in the control is probably underestimated. The pattern of ρ versus μ indicates a higher share of ρ_m during winter conditions (Figure 3B), matching observed field value in April (1.8 fmol O_2 cell^{-1} d^{-1}, ±0.45 95% CI) (Vikström & Wikner, 2019).

Independent effects of temperature and nutrient addition

Previous mesocosm studies have provided important insight into the influence of increased temperatures on driving increases in PG and PR of winter microbial assemblages (Hoppe et al., 2008; von Scheibner et al., 2014). Our results confirmed that temperature was a prime and independent controlling factor in regulating the prokaryotic metabolic processes measured here, except for specific respiration (Table 2). Previous results of nutrient amendment experiments from temperate regions indicate that organic substrates (glucose, dissolved free amino acids, and plankton extract) enhance heterotrophic metabolism more than inorganic substrates (NH_4^+, PO_4^{3-}) (Church et al., 2000; Kirchman, 1990, 2000). Natural nutrient sources consist of exuded organic and inorganic substrates, with yeast extract resembling the former (Catala et al., 2021; Sundh, 1992). Active remineralization by protozoo- and metazooplankton probably also played a role in our experiment, providing nutrients and organic substrates from consumed prey. The different responses to temperature observed for PR and ρ can be related to the significant positive effect of temperature on PA. A higher PA has been reported from the field during the summer season in the same sea area and explained by an increase in carrying capacity at higher temperatures (Wikner & Hagström, 1999, table 3). Significant interaction effects of temperature and nutrients on PG or μ could not be demonstrated in this study, as in some other studies (Felip et al., 1996; Yager & Deming, 1999). This means that temperature and nutrients had a stimulating effect on the studied quantities irrespective of the level of the other. Pomeroy et al. (1991) reported a larger effect on measured respiration by nutrients at cold temperature using sea water cultures in vials. Indeed, ρ in our study showed a tendency of a similar effect, albeit not statistically significant (Figure 2A). The higher ρ at low temperatures is in accordance with observations of the controls and field studies in late winter (Vikström & Wikner, 2019). This can be explained by a strategy of organisms in general to increase their intracellular adenosine triphosphate (ATP) concentrations at low temperatures (Amato & Christner, 2009).

Positive relationship between PGE, μ and PG

The PGE values in the control (Figure S1c and Table S2) were slightly higher than the values observed during oligotrophic field conditions (mean PGE: 2%–7%; Kirchman et al., 2009; Ortega-Retuerta et al., 2012; Reinthaler et al., 2006). The PGE values in the TN treatment were close to estimates from the

productive mesotrophic system (PGE range: 9%–52%; Carlson et al., 1999; Smith & Prairie, 2004). Lower PGE values indicate that prokaryotic communities allocate more carbon and energy for sustaining maintenance activities. Furthermore, lower μ values in the control mean higher maintenance costs compared to the TN treatment according to Figure 4. The addition of nutrients at lower temperatures had a significant effect on PGE compared to additions at higher temperatures, suggesting that higher temperature obscures the effect of nutrient amendments. We hypothesize that elevated temperatures led to an increased amount of bioavailable organic compounds by reducing the activation energy required for catabolism of natural substrates by prokaryotes (Figure 5A). It is noteworthy that the increase in temperature to 10°C alone (T treatment) mobilized a natural substrate pool with nutritional value comparable to that when yeast extract was also supplied (Figures 1A and 5A). Our results further refute the model suggesting an inverse temperature-PGE relationship (Rivkin & Legendre, 2001) while supporting the model that PGE is promoted by prokaryotic productivity and the availability of organic carbon and nutrients (Figures 5B,C) (del Giorgio & Cole, 1998; Roland & Cole, 1999). This may be explained by differences in the scales of investigations, as cross-ecosystem analyses over several latitudes using temperature are confounded with productivity levels. The realistic temperature range between 1 and 10°C in our study is also a reason for a positive relationship, as this is more likely to occur below 20°C (Apple et al., 2006). The shift from 1 to 10°C in our treatments resulted in a significant positive effect on PGE, while a tendency towards a positive nutrient effect was indicated, especially at low temperature (Table 2 and Figure 5A). A positive relationship between PGE and μ ($n = 94$) is also in line with observations in continuous culture systems (Figure 5B) (Middelboe et al., 1992). This observed positive relationship was demonstrated for the whole community and individually for each treatment, except in the control with low variability in prokaryotic variables (Figure 5B and Table S3). In the T and TN treatments the average temporal variation was higher for prokaryotic growth (8.7-fold) than for prokaryotic respiration (5-fold) during the experiment (Figures S1a and S2b). This indicated that the PGE variation in our study was influenced mainly by variation in prokaryotic growth.

del Giorgio and Cole (1998) did not find a relationship between PGE and μ in a cross-ecosystem compilation ($n = 52$). This may be explained by the inevitable influence of different methodologies and environmental conditions in the cross-system comparisons. In our experiment, still covering the global range of PGE values by manipulating temperature and nutrient levels, we demonstrated a positive significant relationship between PGE and μ, both in the individual treatments and the combined dataset (Figure 5B and Table S3). Furthermore, and in accordance with del Giorgio and Cole (1998), we corroborated the nonlinear relationship between PGE and PG for all the treatments (Figure 5C). However, a square root function (Equation 3) showed a better fit to our data (Table S3) than the nonlinear model reported by del Giorgio and Cole (1998) ($r^2 = 0.70$, Table S3). Their model, being derived from field observations including rivers, oceans, lakes, and estuaries, still explained >50% of the variability in our data. This was a further indication that the conditions for prokaryotic growth and metabolism attained in our mesocosm system corresponded to conditions prevalent in natural ecosystems.

Interactive forcing of prokaryotic community composition

Temperature and nutrients markedly influenced the prokaryotic community composition. Each of these factors alone drove succession in different directions over time, and when combined, they induced a more rapid succession and caused a community different from those found in mesocosms exposed to either factor alone. This observation complements recent findings on single and combined effects of factors like temperature, nutrients, and acidification in shaping the aquatic microbiomes (Lindh et al., 2013; Suleiman et al., 2021). These findings collectively suggest that effects on prokaryotic community composition can be markedly different if factors work alone or in concert.

Two interrelated questions emerged that are relevant to consider for interpreting the community composition analysis: (i) How similar was the community composition in the experiment as compared to the natural environment and (ii) Did the community succession in the mesocosms match the winter to summer transitions in the Baltic? Throughout the experiment, the prokaryotic community in the mesocosms included a representative set of major taxa that are found in the Baltic Sea, for example, *Actinobacteria*, *Gammaproteobacteria* and *Bacteroidia*, and this was the case also for several orders and families (Camarena-Gómez et al., 2021; Lindh et al., 2015; Lindh & Pinhassi, 2018). However, it is important to recognize that community composition in natural waters is highly dynamic at a variety of timescales, even down to days and weeks (Bunse & Pinhassi, 2017; Galand et al., 2018; Martin-Platero et al., 2018; Yeh & Fuhrman, 2022). Therefore, and given the paucity of seasonally resolved studies from the Baltic, it is difficult to assess precisely if—or to what extent—the changes in the mesocosms corresponded to changes that would occur for example in the transition from winter to spring/early summer in the field. Nevertheless, we think the maintenance of a broad diversity in the mesocosms, with different key players in the different treatments, indicated that the

dynamics in prokaryotic community could be informative for interpreting successional dynamics. In the following, we relate our observations to what is known about the ecology and physiology of individual taxa.

The observed dynamics induced by nutrients and temperature involved several major taxa. Within the *Betaproteobacteria*, the prominence of the family *Methylophilaceae* in the C-treatment was noteworthy in that it positively correlated with the share of maintenance respiration. *Methylophilaceae* specializes in the metabolism of substrates with no carbon–carbon bonds (C1 compounds, such as methanol and methylated amines) with high carbon conversion efficiency (Windass et al., 1980). This high carbon conversion efficiency of *Methylophilaceae* in oligotrophic systems might be relevant both for anabolic (growth) or catabolic (respiration) reactions and provide a competitive advantage at a low supply of carbon substrates.

Previous 16S rRNA gene analysis from another mesocosm system showed increased occurrence of *Flavobacteriaceae* and *Betaproteobacteria* at a temperature of 6°C in contrast to 0°C (von Scheibner et al., 2014) In our work, the occurrence of *Flavobacteriaceae* was higher in treatments with added organic nutrients (N and TN treatment), especially at low temperatures (N-treatment). Accordingly, this family is known to encode genes associated with the degradation of phytoplankton-derived matter (Bennke et al., 2016; Gavriilidou et al., 2020; Mann et al., 2013). The higher abundances of *Nitrincolaceae* in the treatments with elevated temperatures (T and TN treatment) were another noteworthy effect. *Nitrincolaceae* share the same strategy for carbon acquisition as *Methylophilaceae*, which is associated with the degradation of small molecules and C1 metabolism (Francis et al., 2021). The predominance of *Ilumatobacteraceae* in the C and T treatments coupled with decreased abundance in treatments with nutrient additions (N and TN treatment) suggests a preference for natural substrates supplied in the bulk water and that they are outcompeted by other taxa when labile organic nutrients are available.

The presence of *Burkholderiaceae* in all treatments is consistent with previous Baltic Sea mesocosm observations of *Betaproteobacteria* becoming abundant (Lindh et al., 2013). Compared to the stable family-level dynamics, *Burkholderiaceae* exhibited pronounced dynamics at the level of individual ASVs (Figure S2). For example, the major *Burkholderiaceae* population in the N-treatment, ASV4, belonged to the genus *Rhodoferax*, whereas ASV6, which became dominant in the controls, was affiliated with the genus *Polaromonas*, which is known to encompass psychrotolerant strains (Ciok et al., 2018). In both treatments with elevated temperature, ASV2 (genus unclassified) was instead the prominent *Burkholderiaceae*, suggesting a selective forcing based on temperature within the family. This is also consistent with the observation that temperatures of approximately 6°C or higher may cause a loss of some psychrotolerants (Lindh et al., 2013). It can be noted that archaeal ASVs were observed, but not abundant, matching the observation of archaeal presence in winter surface waters (occasionally at relative abundance up to 12%) in the Baltic Proper (Lindh et al., 2015).

A complimentary view on ASV responses in our experiment was the temporal succession within the *Flavobacteriaceae* in the N-treatment. Such successions within the *Flavobacteriaceae* have been shown in relation to spring phytoplankton blooms (Lindh et al., 2015) and might be induced by a succession in substrate availability (Teeling et al., 2012). Also in the TN-treatment, there was a pronounced succession of ASVs, although in this case the ASVs spanned a variety of families. Taken together, significant differences in prokaryotic community composition were demonstrated, making taxon-specific metabolisms a candidate to explain some of the differences in maintenance respiration observed between the treatments.

AUTHOR CONTRIBUTIONS

AV contributed to design of the study, sampling mesocosm, measured abundance and made most statistical analyses on abundance, growth and respiration, and was main autor of the manuscript. DA performed sampling of prokaryote diversity, made the bioinfomatics, statistical analysis of those, and wrote the corresponding section. JP designed and quality assured the study of diversity, supervised bioinformatic analyses, and contributed to writing of the manuscript. JW designed the factorial experiment, measured growth rate, made quality assurance, designed statistical analyses of treatment effects and trendanalyses, and wrote the manuscript.

ACKNOWLEDGEMENTS

The authors acknowledge the technical and analytical support from the staff at Ume Marine Science Centre (UMF). Annie Marie Cox for respiration measurements and general mesocosm support together with Mikael Molin. Mikael Peedu contributed to prokaryotic growth rate measurements. The authors thank the National Genomics Infrastructure (NGI) platform at SciLifeLab, Sweden for sequencing and Anders Jonsson at the Biogeochemical Analytical Facility (BAF) at Umeå University for laboratory assistance. This study was funded by the Kempe Foundation (SMK-185) and the Eco-Change strategic research program (Johan Wikner). Two trainees were supported by the Transnational Access program of the EU H2020-INFRAIA project (No. 731065) AQUACOSM—Network of Leading European AQUAtic MesoCOSM Facilities Connecting Mountains to Oceans from the Arctic to the Mediterranean—funded by the European Commission.

This is a contribution from Umeå Center for Microbial Research.

CONFLICT OF INTEREST

The authors have no conflicts of interest to declare.

DATA AVAILABILITY STATEMENT

The ecological data set is available at the Pangea repository (https://www.pangea.de) identity code PDI-33690. DNA sequences of the 16S rRNA gene amplicons are available from the NCBI Sequence Read Archive under BioProject no. PRJNA796754, accession no. SRR17595721-SRR17595816. All codes for metabarcoding are available at https://github.com/dennisamne/promac_16 S.

REFERENCES

Alonso-Sáez, L., Gasol, J.M., Arístegui, J., Vilas, J.C., Vaqué, D., Duarte, C.M. et al. (2007) Large-scale variability in surface bacterial carbon demand and growth efficiency in the subtropical Northeast Atlantic ocean. *Limnology and Oceanography*, 52, 533–546.

Amato, P. & Christner, B.C. (2009) Energy metabolism response to low-temperature and frozen conditions in *Psychrobacter cryohalolentis*. *Applied and Environmental Microbiology*, 75, 711–718.

Andrews, S. (2011) *FastQC: a quality control tool for high throughput sequence data*. Cambridge, MA: Babraham Institute.

Apple, J.K., Del Giorgio, P.A. & Kemp, W.M. (2006) Temperature regulation of bacterial production, respiration, and growth efficiency in a temperate salt-marsh estuary. *Aquatic Microbial Ecology*, 43, 243–254.

Bennke, C.M., Kruger, K., Kappelmann, L., Huang, S., Gobet, A., Schuler, M. et al. (2016) Polysaccharide utilisation loci of Bacteroidetes from two contrasting open ocean sites in the North Atlantic. *Environmental Microbiology*, 18, 4456–4470.

Berggren, M., Laudon, H., Jonsson, A. & Jansson, M. (2010) Nutrient constraints on metabolism affect the temperature regulation of aquatic bacterial growth efficiency. *Microbial Ecology*, 60, 894–902.

Blackburn, N., Hagström, Å., Wikner, J., Cuadros-Hansson, R. & Bjornsen, P.K. (1998) Rapid determination of bacterial abundance, biovolume, morphology, and growth by neural network-based image analysis. *Applied and Environmental Microbiology*, 64, 3246–3255.

Bolyen, E., Rideout, J.R., Dillon, M.R., Bokulich, N.A., Abnet, C.C., Al-Ghalith, G.A. et al. (2019) Reproducible, interactive, scalable and extensible microbiome data science using QIIME 2. *Nature Biotechnology*, 37, 852–857.

Bunse, C. & Pinhassi, J. (2017) Marine bacterioplankton seasonal succession dynamics. *Trends in Microbiology*, 25, 494–505.

Cajal-Medrano, R. & Maske, H. (1999) Growth efficiency, growth rate and the remineralization of organic substrate by bacterioplankton - revisiting the Pirt model. *Aquatic Microbial Ecology*, 19, 119–128.

Callahan, B.J., McMurdie, P.J., Rosen, M.J., Han, A.W., Johnson, A. J. & Holmes, S.P. (2016) DADA2: high-resolution sample inference from Illumina amplicon data. *Nature Methods*, 13, 581–583.

Camarena-Gómez, M.T., Ruiz-González, C., Piiparinen, J., Lipsewers, T., Sobrino, C., Logares, R. et al. (2021) Bacterioplankton dynamics driven by interannual and spatial variation in diatom and dinoflagellate spring bloom communities in the Baltic Sea. *Limnology and Oceanography*, 66, 255–271.

Carlson, C.A., Bates, N.R., Ducklow, H.W. & Hansell, D.A. (1999) Estimation of bacterial respiration and growth efficiency in the Ross Sea, Antarctica. *Aquatic Microbial Ecology*, 19, 229–244.

Carstensen, J., Andersen, J.H., Gustafsson, B.G. & Conley, D.J. (2014) Deoxygenation of the Baltic Sea during the last century. *Proceedings of the National Academy of Sciences of the United States of America*, 111, 5628–5633.

Catala, T.S., Shorte, S. & Dittmar, T. (2021) Marine dissolved organic matter: a vast and unexplored molecular space. *Applied Microbiology and Biotechnology*, 105, 7225–7239.

Church, M.J., Hutchins, D.A. & Ducklow, H.W. (2000) Limitation of bacterial growth by dissolved organic matter and iron in the Southern Ocean. *Applied and Environmental Microbiology*, 66, 455–466.

Ciok, A., Budzik, K., Zdanowski, M.K., Gawor, J., Grzesiak, J., Decewicz, P. et al. (2018) Plasmids of psychrotolerant *Polaromonas* spp. isolated from Arctic and Antarctic glaciers - diversity and role in adaptation to polar environments. *Frontiers in Microbiology*, 9, 1285.

del Giorgio, P.A. (2000) Bacterial energetics and growth efficiency. In: Kirchman, D. (Ed.) *Microbial ecology of the oceans*. New York, NY: Wiley, pp. 289–325.

del Giorgio, P.A. & Cole, J.J. (1998) Bacterial growth efficiency in natural aquatic systems. *Annual Review of Ecology and Systematics*, 29, 503–541.

del Giorgio, P.A., Condon, R., Bouvier, T., Longnecker, K., Bouvier, C., Sherr, E. et al. (2011) Coherent patterns in bacterial growth, growth efficiency, and leucine metabolism along a Northeastern Pacific inshore-offshore transect. *Limnology and Oceanography*, 56, 1–16.

Diaz, R.J. & Rosenberg, R. (2008) Spreading dead zones and consequences for marine ecosystems. *Science*, 321, 926–929.

Ewels, P., Magnusson, M., Lundin, S. & Kaller, M. (2016) MultiQC: summarize analysis results for multiple tools and samples in a single report. *Bioinformatics*, 32, 3047–3048.

Felip, M., Pace, M.L. & Cole, J.J. (1996) Regulation of planktonic bacterial growth rates: the effect of temperature and resources. *Microbial Ecology*, 31, 15–28.

Francis, B., Urich, T., Mikolasch, A., Teeling, H. & Amann, R. (2021) North Sea spring bloom-associated Gammaproteobacteria fill diverse heterotrophic niches. *Environmental Microbiome*, 16, 15.

Fuhrman, J.A. & Azam, F. (1982) Thymidine incorporation as a measure of heterotrophic bacterioplankton production in marine surface waters: evaluation and field results. *Marine Biology*, 66, 109–120.

Galand, P.E., Pereira, O., Hochart, C., Auguet, J.C. & Debroas, D. (2018) A strong link between marine microbial community composition and function challenges the idea of functional redundancy. *The ISME Journal*, 12, 2470–2478.

Gasol, J.M., Doval, M.D., Pinhassi, J., Calderón-Paz, J.I., Guixa-Boixareu, N., Vaqué, D. et al. (1998) Diel variations in bacterial heterotrophic activity and growth in the Northwestern Mediterranean sea. *Marine Ecology Progress Series*, 164, 107–124.

Gavriilidou, A., Gutleben, J., Versluis, D., Forgiarini, F., van Passel, M.W.J., Ingham, C.J. et al. (2020) Comparative genomic analysis of *Flavobacteriaceae*: insights into carbohydrate metabolism, gliding motility and secondary metabolite biosynthesis. *BMC Genomics*, 21, 569.

Grasshoff, K., Kremling, K. & Ehrhardt, M. (1999) *Methods of seawater analysis*. Weinheim: John Wiley & Sons.

Herlemann, D.P.R., Labrenz, M., Jürgens, K., Bertilsson, S., Waniek, J.J. & Andersson, A.F. (2011) Transitions in bacterial communities along the 2000 km salinity gradient of the Baltic sea. *The ISME Journal*, 5, 1571–1579.

Hobbie, J.E., Daley, R.J. & Jasper, S. (1977) Use of nuclepore filters for counting bacteria by fluorescence microscopy. *Applied and Environmental Microbiology*, 33, 1225–1228.

Hoppe, H.G., Breithaupt, P., Walther, K., Koppe, R., Bleck, S., Sommer, U. et al. (2008) Climate warming in winter affects the coupling between phytoplankton and bacteria during the spring bloom: results from a mesocosm study. *Aquatic Microbial Ecology*, 51, 105–115.

Hugerth, L.W., Wefer, H.A., Lundin, S., Jakobsson, H.E., Lindberg, M., Rodin, S. et al. (2014) DegePrime, a program for degenerate primer design for broad taxonomic-range PCR in microbial ecology studies. *Applied and Environmental Microbiology*, 80, 5116–5123.

Kirchman, D.L. (1990) Limitation of bacterial growth by dissolved organic matter in the subarctic Pacific. *Marine Ecology Progress Series*, 62, 47–54.

Kirchman, D.L. (2000) Uptake and regeneration of inorganic nutrients by marine heterotrophic bacteria. In: Kirchman, D.L. (Ed.) *Microbial ecology of the oceans*. New York, NY: Wiley-Liss, pp. 261–288.

Kirchman, D.L. (2016) Growth rates of microbes in the oceans. *Annual Review of Marine Science*, 8, 285–309.

Kirchman, D.L., Hill, V., Cottrell, M.T., Gradinger, R., Malmstrom, R. R. & Parker, A. (2009) Standing stocks, production, and respiration of phytoplankton and heterotrophic bacteria in the Western Arctic ocean. *Deep-Sea Research Part II: Oceanographic Research Papers*, 56, 1237–1248.

Kolde, R. (2019) pheatmap: Pretty Heatmaps. R Package Version 1.0.12. https://CRAN.R-project.org/package=pheatmap

Lee, C.W., Bong, C.W. & Hii, Y.S. (2009) Temporal variation of bacterial respiration and growth efficiency in tropical coastal waters. *Applied and Environmental Microbiology*, 75, 7594–7601.

Lindh, M.V. & Pinhassi, J. (2018) Sensitivity of bacterioplankton to environmental disturbance: a review of Baltic Sea field studies and experiments. *Frontiers in Marine Science*, 5, 1–17.

Lindh, M.V., Riemann, L., Baltar, F., Romero-Oliva, C., Salomon, P. S., Granéli, E. et al. (2013) Consequences of increased temperature and acidification on bacterioplankton community composition during a mesocosm spring bloom in the Baltic sea. *Environmental Microbiology Reports*, 5, 252–262.

Lindh, M.V., Sjöstedt, J., Andersson, A.F., Baltar, F., Hugerth, L.W., Lundin, D. et al. (2015) Disentangling seasonal bacterioplankton population dynamics by high-frequency sampling. *Environmental Microbiology*, 17, 2459–2476.

López-Urrutia, Á. & Morán, X.A.G. (2007) Resource limitation of bacterial production distorts the temperature dependence of oceanic carbon cycling. *Ecology*, 88, 817–822.

Mann, A.J., Hahnke, R.L., Huang, S., Werner, J., Xing, P., Barbeyron, T. et al. (2013) The genome of the alga-associated marine flavobacterium *Formosa agariphila* KMM 3901T reveals a broad potential for degradation of algal polysaccharides. *Applied and Environmental Microbiology*, 79, 6813–6822.

Maranger, R.J., Pace, M.L., Del Giorgio, P.A., Caraco, N.F. & Cole, J. J. (2005) Longitudinal spatial patterns of bacterial production and respiration in a large river-estuary: implications for ecosystem carbon consumption. *Ecosystems*, 8, 318–330.

Martin, M. (2011) Cutadapt removes adapter sequences from high-throughput sequencing reads. *EMBnetJournal*, 17, 10–12.

Martin-Platero, A.M., Cleary, B., Kauffman, K., Preheim, S.P., McGillicuddy, D.J., Alm, E.J. et al. (2018) High resolution time series reveals cohesive but short-lived communities in coastal plankton. *Nature Communications*, 9, 1–11.

Middelboe, M., Nielsen, B. & Søndergaard, M. (1992) Bacterial utilization of dissolved organic carbon (DOC) in coastal waters—determination of growth yield. *Archiv für Hydrobiologie. Beihefte. Ergebnisse der Limnologie*, 37, 51–61.

Norland, S. (1993) The relationship between biomass and volume of bacteria. In: *Handbook of methods in aquatic microbial ecology*. Boca Raton: CRC press, pp. 303–307.

Norrman, B. (1993) Filtration of water samples for DOC studies. *Marine Chemistry*, 41, 239–242.

Obernosterer, I., Christaki, U., Lefèvre, D., Catala, P., Van Wambeke, F. & Lebaron, P. (2008) Rapid bacterial mineralization of organic carbon produced during a phytoplankton bloom induced by natural iron fertilization in the southern ocean. *Deep-Sea Research Part II: Oceanographic Research Paper*, 55, 777–789.

Oksanen, J., Blanchet, F.G., Friendly, M., Kindt, R., Legendre, P., McGlinn, D. et al. (2020) Package "vegan". Community ecology package version 2.5-7. https://github.com/vegandevs/vegan

Ortega-Retuerta, E., Jeffrey, W.H., Babin, M., Bélanger, S., Benner, R., Marie, D. et al. (2012) Carbon fluxes in the Canadian Arctic: patterns and drivers of bacterial abundance, production and respiration on the Beaufort Sea margin. *Biogeosciences*, 9, 3679–3692.

Pedrós-Alió, C., Calderón-Paz, J.-I., Guixa-Boixereu, N., Estrada, M. & Gasol, J.M. (1999) Bacterioplankton and phytoplankton biomass and production during summer stratification in the Northwestern Mediterranean sea. *Deep Sea Research Part I: Oceanographic Research Papers*, 46, 985–1019.

Pirt, S.J. (1982) Maintenance energy: a general model for energy-limited and energy-sufficient growth. *Archives of Microbiology*, 133, 300–302.

Pomeroy, L.R. & Wiebe, W.J. (2001) Temperature and substrates as interactive limiting factors for marine heterotrophic bacteria. *Aquatic Microbial Ecology*, 23, 187–204.

Pomeroy, L.R., Wiebe, W.J., Deibel, D., Thompson, R.J., Rowe, G. T. & Pakulski, J.D. (1991) Bacterial responses to temperature and substrate concentration during the Newfoundland spring bloom. *Marine Ecology Progress Series*, 75, 143–159.

Quast, C., Pruesse, E., Yilmaz, P., Gerken, J., Schweer, T., Yarza, P. et al. (2013) The SILVA ribosomal RNA gene database project: improved data processing and web-based tools. *Nucleic Acids Research*, 41, D590–D596.

R Development Core Team. (2020) The R Project for Statistical Computing Version 3.6.3. https://www.r-project.org

Reinthaler, T., Van Aken, H., Veth, C., Arístegui, J., Robinson, C., Williams, P.J.L.B. et al. (2006) Prokaryotic respiration and production in the meso- and bathypelagic realm of the eastern and western North Atlantic basin. *Limnology and Oceanography*, 51, 1262–1273.

Rivkin, R.B. & Legendre, L. (2001) Biogenic carbon cycling in the upper ocean: effects of microbial respiration. *Science*, 291, 2398–2400.

Robinson, C. & Williams, P.J.B. (2005) Respiration and its measurement in surface marine waters. In: del Giorgio, P.A. & Williams, P.J.B. (Eds.) *Respiration in aquatic ecosystems*. Oxford, UK: Oxford University Press, pp. 147–180.

Roland, F. & Cole, J.J. (1999) Regulation of bacterial growth efficiency in a large turbid estuary. *Aquatic Microbial Ecology*, 20, 31–38.

Russell, J.B. (2007) The energy spilling reactions of bacteria and other organisms. *Journal of Molecular Microbiology and Biotechnology*, 13, 1–11.

Schimel, J., Balser, T.C. & Wallenstein, M. (2007) Microbial stress-response physiology and its implications for ecosystem function. *Ecology*, 88, 1386–1394.

Schmidtko, S., Stramma, L. & Visbeck, M. (2017) Decline in global oceanic oxygen content during the past five decades. *Nature*, 542, 335–339.

Shiah, F.-K. & Ducklow, H.W. (1994) Temperature and substrate regulation of bacterial abundance, production and specific growth rate in Chesapeake Bay, USA. *Marine Ecology Progress Series*, 103, 297–308.

Simon, M. & Azam, F. (1989) Protein content and protein synthesis rates of planktonic marine bacteria. *Marine Ecology Progress Series*, 51, 201–213.

SMHI. (2020) Swedish Meteorological and Hydrological Institute. https://www.smhi.se/en/services/open-data/search-smhi-s-open-data-1.81004

Smith, E.M. & Prairie, Y.T. (2004) Bacterial metabolism and growth efficiency in lakes: the importance of phosphorus availability. *Limnology and Oceanography*, 49, 137–147.

Straub, D., Blackwell, N., Langarica-Fuentes, A., Peltzer, A., Nahnsen, S. & Kleindienst, S. (2020) Interpretations of environmental microbial community studies are biased by the selected 16S rRNA (gene) amplicon sequencing pipeline. *Frontiers in Microbiology*, 11, 550420.

Sugimura, Y. & Suzuki, Y. (1988) A high-temperature catalytic oxidation method for the determination of non-volatile dissolved organic carbon in seawater by direct injection of a liquid sample. *Marine Chemistry*, 24, 105–131.

Suleiman, M., Choffat, Y., Daugaard, U. & Petchey, O.L. (2021) Large and interacting effects of temperature and nutrient addition on stratified microbial ecosystems in a small, replicated, and liquid-dominated Winogradsky column approach. *Microbiology*, 10, e1189.

Sundh, I. (1992) Biochemical composition of dissolved organic carbon derived from phytoplankton and used by heterotrophic bacteria. *Applied and Environmental Microbiology*, 58, 2938–2947.

Teeling, H., Fuchs, B.M., Becher, D., Klockow, C., Gardebrecht, A., Bennke, C.M. et al. (2012) Substrate-controlled successionof marine bacterioplankton populations induced by a phytoplankton bloom. *Science*, 336, 608–611.

Toolan, T. (2001) Coulometric carbon‐based respiration rates and estimates of bacterioplankton growth efficiencies in Massachusetts Bay. *Limnology and Oceanography*, 46, 1298–1308.

van Bodegom, P. (2007) Microbial maintenance: a critical review on its quantification. *Microbial Ecology*, 53, 513–523.

Vikström, K. & Wikner, J. (2019) Importance of bacterial maintenance respiration in a subarctic estuary: a proof of concept from the field. *Microbial Ecology*, 77, 574–586.

von Scheibner, M., Dörge, P., Biermann, A., Sommer, U., Hoppe, H. G. & Jürgens, K. (2014) Impact of warming on phytobacterioplankton coupling and bacterial community composition in experimental mesocosms. *Environmental Microbiology*, 16, 718–733.

von Scheibner, M., Herlemann, D.P.R., Lewandowska, A.M. & Jürgens, K. (2018) Phyto-and bacterioplankton during early spring conditions in the Baltic sea and response to short-term experimental warming. *Frontiers in Marine Science*, 5, 1–13.

Wickham, H. (2016) *ggplot2: elegant graphics for data analysis*. New York, NY: Springer-Verlag.

Wikner, J. & Hagström, Å. (1999) Bacterioplankton intra-annual variability: importance of hydrography and competition. *Aquatic Microbial Ecology*, 20, 245–260.

Wikner, J., Panigrahi, S., Nydahl, A., Lundberg, E., Båmstedt, U. & Tengberg, A. (2013) Precise continuous measurements of pelagic respiration in coastal waters with oxygen optodes. *Limnology and Oceanography: Methods*, 11, 1–15.

Windass, J., Worsey, M., Pioli, E., Pioli, D., Barth, P., Atherton, K. et al. (1980) Improved conversion of methanol to single-cell protein by *Methylophilus methylotrophus*. *Nature*, 287, 396–401.

Wohlers, J., Engel, A., Zöllner, E., Breithaupt, P., Jürgens, K., Hoppe, H.G. et al. (2009) Changes in biogenic carbon flow in response to sea surface warming. *Proceedings of the National Academy of Sciences of the United States of America*, 106, 7067–7072.

Wohlers-Zöllner, J., Biermann, A., Engel, A., Dörge, P., Lewandowska, A.M., von Scheibner, M. et al. (2012) Effects of rising temperature on pelagic biogeochemistry in mesocosm systems: a comparative analysis of the AQUASHIFT Kiel experiments. *Marine Biology*, 159, 2503–2518.

Yager, P.L. & Deming, J.W. (1999) Pelagic microbial activity in an arctic polynya: testing for temperature and substarte interactions using a kinetic approach. *Limnology and Oceanography*, 44, 1882–1893.

Yeh, Y.-C. & Fuhrman, J.A. (2022) Contrasting diversity patterns of prokaryotes and protists over time and depth at the san-Pedro ocean time series. *ISME Communications*, 2, 1–12.

SUPPORTING INFORMATION

Additional supporting information can be found online in the Supporting Information section at the end of this article.

How to cite this article: Verma, A., Amnebrink, D., Pinhassi, J. & Wikner, J. (2023) Prokaryotic maintenance respiration and growth efficiency field patterns reproduced by temperature and nutrient control at mesocosm scale. *Environmental Microbiology*, 25(3), 721–737. Available from: https://doi.org/10.1111/1462-2920.16300